Ultrastructural hepatocytic alterations induced by silver nanoparticle toxicity

Mansour Almansour PhD, Laszlo Sajti PhD, Walid Melhim MSc & Bashir M. Jarrar PhD

Published online: 02 Mar 2016.

Submit your article to this journal ⌁

View related articles ⌁

View Crossmark data ⌁

Taylor & Francis
Taylor & Francis Group

Ultrastructural hepatocytic alterations induced by silver nanoparticle toxicity

Mansour Almansour, PhD[a], Laszlo Sajti, PhD[b], Walid Melhim, MSc[c], and Bashir M. Jarrar, PhD[d]

[a]Department of Zoology, College of Science, King Saud University, Saudi Arabia; [b]Nanotechnology Department, Laser Zentrum-Hannover, Hannover, Germany; [c]Electron Microscopy Unit, College of Medicine, King Faisal University, Saudi Arabia; [d]Department of Biological Sciences, College of Science, Jerash University, Jordan

ABSTRACT

Silver nanoparticles (SNPs) are widely used in nanomedicine and consuming products with potential risk on human health. While considerable work was carried out on the molecular, biochemical, and physiological alterations induced by these particles, little is known of the ultrastructural pathological alterations that might be induced by nanosilver materials. The aim of the present work is to investigate the hepatocyte ultrastructural alterations that might be induced by SNP exposure. Male rats were subjected to a daily single dose (2 mg/kg) of SNPs (15–35 nm diameter) for 21 days. Liver biopsies from all rats under study were processed for transmission electron microscopy examination. The following hepatic ultrastructural alterations were demonstrated: mitochondria swelling and crystolysis, endoplasmic reticulum disruption, cytoplasmic vacuolization, lipid droplets accumulation, glycogen depletion, karyopyknosis, apoptosis, sinusoidal dilatation, Kupffer cells activation, and myelin figures formation. The current findings may indicate that SNPs can induce hepatocyte organelles alteration, leading to cellular damage that may affect the function of the liver. These findings might indicate that SNPs potentially trigger heptocyte ultrastructural alterations that may affect the function of the liver with potential risk on human health in relation to numerous applications of these particles. More work is needed to elucidate probable ultrastructural alterations in the vital organs that might result from nanosilver toxicity.

Introduction

Silver nanoparticles (SNPs) have been rapidly involved in nanomedicine, consuming products, and environmental issues due to their unique antimicrobial, antifungal, and antiviral properties [1,2]. While the number of commercial and industrial products employing SNPs was 30 in 2006, it has grown to 1300 by the beginning of 2014 in various applications in one way or another [3]. SNPs have been widely used in alginate fibers and wound dressing in treating wounds, burns, skin ulcers, and catheter-related infections [4,5]. Furthermore, nanosilver is also used in coating medical instruments and tools together with commercial brands of sunscreen, medical masks, gels, cosmetics, bone cement, tooth paste, deodorants, dental resin composite, and shampoo [5]. Moreover, these fine particles are invested in medical cloth, footwear, athletic shirts, and textile manufacturing to limit odor due to sweating [6,7]. In addition, SNPs have unique optical, electrical, and thermal properties and are being used in biological and chemical sensors [8].

The smaller nature of SNPs together with their high surface area to mass ratio enables them to penetrate the cell easily by diffusion or endocytosis as biological molecules do [9,10]. Their toxicity might be related to the charge and functional groups on the surface of these particles and due to the release of silver ions. The released ions are neutralized by binding or interacting with the cell component leading to depletion of dissolved oxygen and generating reactive oxygen

species (ROS) together with reactive nitrogen species (RNS) leading to molecular and biochemical alterations [11–17]. *In vitro* toxicological studies showed that SNPs could initiate ROS production that could damage plasma membrane and cell organelles stimulating organelle oxidative damage and cytoskeleton disruption [18]. Moreover, SNPs can also produce cytotoxic RNS with negative impact on the mitochondrial function, membrane integrity, glutathione depletion, and inflammatory cytokine release [19–22]. In addition, SNPs can interact with the cellular proteins with possible adsorption of these molecules at the surface of the particles forming what is known as the nanoparticle-protein corona [23]. The toxicity of SNPs is related with corona composition and associated with the particle size, shape, and surface area [24]. In addition, probable heat alteration due to the plasmonic effect of SNPs might result in conformational changes in the macromolecules of the cell. On the other hand, Asharani et al. [25] concluded that SNPs could induce DNA damage, negatively affect DNA integrity, increase chromosomal aberrations, disturb G2/M cell cycle, and reduce metabolic activity and ATP production in treated cells. Moreover, other toxicological studies have demonstrated size-dependent genotoxic and cytotoxic consequences associated with SNP exposure [20–22].

SNPs can have the same dimensions of the biological molecules, with the possibility of being adsorbed on the surface of these molecules in the tissues and cells [7]. Nanoparticles less than 100 nm in diameter can enter cells, while those less than

---

CONTACT Bashir M. Jarrar ✉ bashirjarrar@yahoo.com ▣ Department of Biological Sciences, College of Science, Jerash University, Jerash 26150, Jordan.
Color versions of one or more of the figures in the article can be found online at www.tandfonline.com/iusp.

40 nm can enter the nucleus [26, 27]. Recent studies indicated that small SNPs were more toxic than the larger ones [28–36]. Particle size-dependent cellular toxicity was reported by Kim et al. [37], where 10 and 20 nm SNPs were more toxic than the larger ones (50 and 100 nm). Other reports indicated that SNPs could stimulate inflammation and oxidative damage affecting cellular metabolism and membrane integrity via lipid peroxidation and protein denaturation [21,38,39].

The liver regulates body metabolism and fight body toxification by many exogenous challenges that make it highly susceptible to their adverse and toxic effects [40]. The hepatocytes form the main parenchymal tissue of the liver are involved in protein, cholesterol, bile salts, and phospholipids synthesis together with the detoxification, transformation, and modification of exogenous and endogenous materials. Some reports explained that SNPs could accumulate mainly in the liver and other vital organs, with the mitochondria as primary organelle target [8,13,28–33]. Moreover, toxicological reports showed that SNPs were capable to induce injuries in the liver, kidney, testes, heart, brain, and lungs [10,28,29]. In addition, some histopathological reports explained that SNPs can induce cytoplasmic accumulation, focal necrosis, bile-duct hyperplasia, fibrosis, edema, and inflammatory cell infiltration in the hepatic tissues [30,32]. Furthermore, SNPs were reported to induce hematological and biochemical alterations, while case studies revealed that some silver-coated wound dressing elevated liver enzymes [33–36]. In addition, exposure to SNPs increased the serum levels of alanine aminotransferase (ALT), aspartate aminotransferase (AST), and alkaline phosphatase together with DNA damage and apoptosis [32,39]. Morphometric and histological hepatic alterations were also induced by 20-nm SNP subjection [10,28,31].

Exposure to SNPs is becoming part of our lives with wide use of these particles in different sectors, making these particles persisted in our environment with possible potential risk to our health. These concerns need to be considered before determination if SNP benefits outweigh their potential risks with special attention needed toward size, composition, and behavior of these particles. Limited information, if any, is available on the ultrastructural alterations induced in the hepatic tissues by SNPs, a concern to be clarified by the present study.

Materials and methods

Animals and conditions

Twenty healthy male Wistar albino rats of King Saud University colony of the same age (10–12 weeks old) weighing 210–230 gm were used. The animals were housed at 24°C ± 1°C, on 12 h light–12 h dark/light cycle, randomly assigned and separately caged to one test group and a control one (10 rats each).

Silver nanoparticles

Spherical SNPs (15–35 nm diameter) dissolved in deionized water containing 0.1 mM sodium citrate were obtained from the Department of Nanotechnology of Laser Zentrum-Hannover, Germany. SNPs were fabricated by picosecond-pulsed

laser ablation in liquids (PLAL). The ablation process was carried as follows: a silver foil (8 × 8 × 0.1 mm; purity: 99.99%, Goodfellow GmbH, Germany) was fixed within a self-constructed ablation chamber made of Teflon which was filled with 35 ml of deionized water containing 0.1 mM sodium citrate, resulting in a liquid column of 10 mm. The laser beam was coupled into a galvanometric scanner laser (HurrySCAN II-14, Scanlab AG Germany), which allowed deposition of laser pulses with controlled interpulse distance on the silver target after focusing with a 56-mm telecentric lens. Liquid stirring was applied using a Teflon rotor for continuous liquid agitation and quick removal of ablated nanoparticles from the process zone. Determination of laser spot size on the target for flounce calculation was performed according to Farkas et al. [41]. Ligand-free SNPs were generated by applying 250 μJ pulse energy with a repetition rate of 33 kHz and laser fluency of 12.7 Jcm^{-2}. Target position was selected with respect to the focus position in air and to yield the highest ablation rate in deionized distilled water. The optical extinction spectra of the fabricated particles were measured by using UV-Vis spectroscopy (Shimadzu 1650), while the nanoparticle micrographs were obtained by the use of a scanning electron microscope (Quanta 400 FEG).

Experimental protocol

Following a period of stabilization (7 days), the control animals received a daily i.p. injection of the vehicle (400 μl deionized water containing 0.1 mM sodium citrate) only, while test group members received a daily i.p. injection of 400 μl of SNPs (2 mg/kg) for 21 days.

All animals were handled and all experiments were conducted in accordance with the protocols approved by King Saud University animal care ethical committee. In addition, the experimental procedures were carried out in accordance with international guidelines for care and use of laboratory animals.

Electron microscopic investigation

Small pieces of liver from each rat minced into small cubes of 1 mm in length were fixed in 2.5% glutaraldehyde fixative in 0.1 M phosphate buffer (pH 7.4) for 24 h at 4°C. Specimens were then post-fixed in 2% osmium tetroxide (OsO_4) in cacodylate buffer for 90 min at room temperature. Tissues were washed in the buffer and dehydrated at 4°C through a gradual series of acetone and embedded in Epon–araldite resin mixture [42–44]. Semithin sections (500–1000 nm) were obtained in a Leica EM UC6 ultramicrotome mounted on glass slides, stained with toluidine blue (1%), examined, and photographed using light microscopy. Ultrathin sections (60 nm thick) were obtained with a diamond knife on Leica EM UC6 ultramicrotome and mounted on 200-mesh hexagonal copper grids, with 0.5% uranyl acetate and 3% lead citrate using the Leica automated EM stainer [45]. Ultrsection examination and structural abnormality evaluation was carried out by using Jeol transmission electron microscope at 80 kv (JEM-1011, Japan).

Results

Silver nanoparticle characterization

As represented in Figure 1(a–c), the used SNPs demonstrated spherical morphology with size variation range of 15–35 nm in diameter where the maximum particle count was at 20 ± 5 nm size. In addition, the UV-visible spectrum of the particles presented single symmetric absorption band with maximum peak of absorbance around ~400 nm that correspond to the normalized absorption spectrum of SNPs.

Control rats

Semithin and ultrathin sections of the control rats demonstrated normal hepatocytes as well as normal sinusoids lined with Kupffer cell. The hepatocytes revealed normal nucleoplasm with nuclei surrounded by even distinct nuclear envelop demonstrating heterochromatin adjacent to the border. The cytoplasm of these hepatocytes appeared crowded with organelles mainly the mitochondria, endoplasmic reticulum (ER), free and bounded ribosomes, lysosomes, and glycogen particles (Figures 2a,b). The control hepatocytes demonstrated mitochondria in orthodox conformation together with regular parallel organized ER.

Rats exposed to 20 nm SNPs

In comparison with the control group, the hepatic tissues of SNP-treated rats exhibited the following remarkable alterations:

- Sinusoidal dilatation: Examination of semithin sections stained with toluidine blue reveals sinusoidal dilation in the hepatic tissues of rats treated with SNPs (Figures 3a, b). Sinusoidal dilatation was also demonstrated in the electron micrograph sections where red blood cells and debris were observed in the dilated sinusoids (Figure 4).
- Alterations in the rough endoplasmic reticulum: Partial destruction and reduction profile together with a loss of arrays, stacks, and shortening of rough ER were demonstrated (Figure 5a). Occasional vesiculated and dilated ER were also seen (Figure 5b). Moreover, degranulation of the rough ER and ribosomal dropping were also observed.
- Mitochondrial alterations: The pleomorphic mitochondria of SNP-treated rats demonstrated swelling, cristolysis,
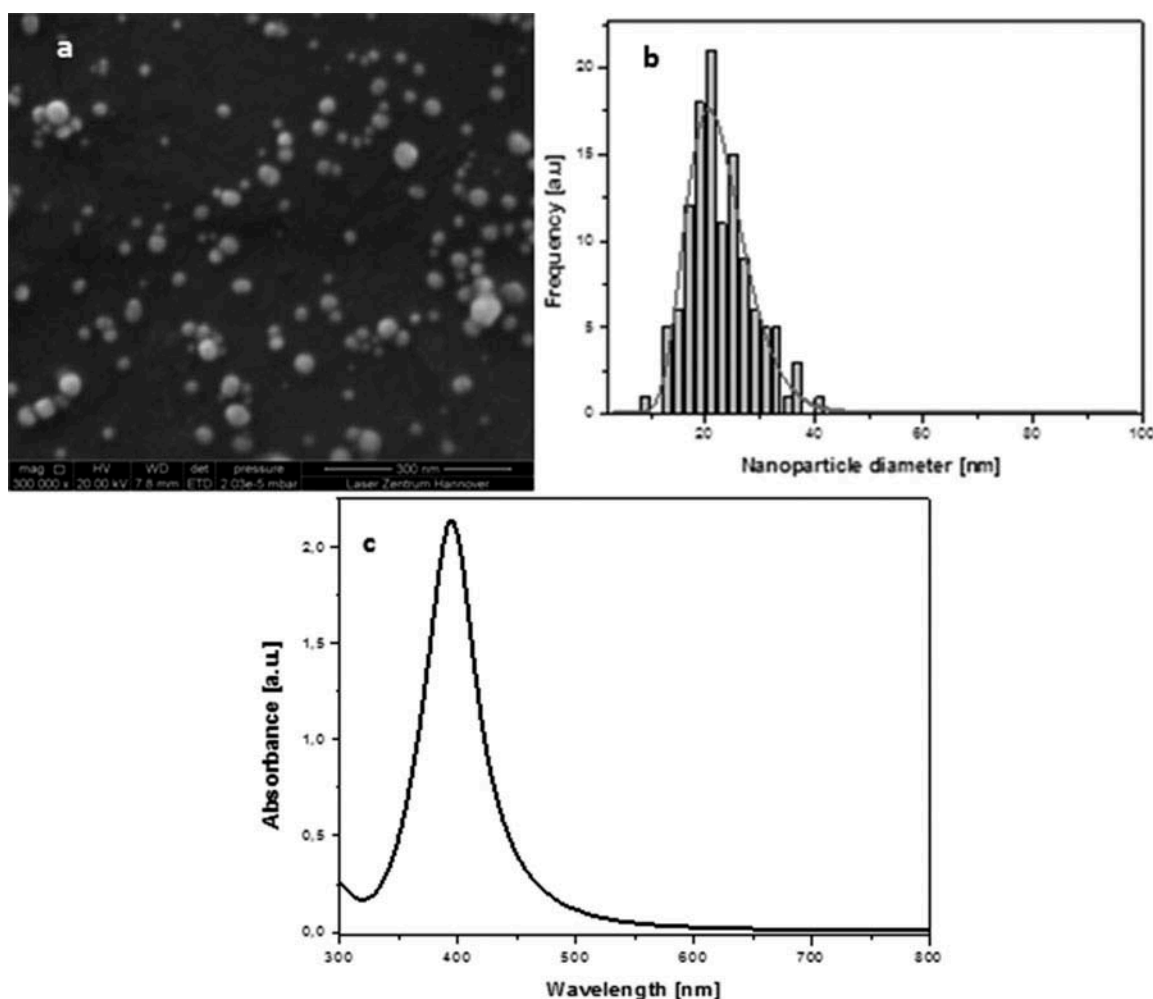

Figure 1. (a–c) Physical characterization of the used SNPs demonstrating: (a) Scanning electron micrograph demonstrating spherical morphology of the used SNPs. (b) Histogram showing that the particle size distribution of the used SNPs is within the range of 15–35 nm in diameter, with maximum particle count at 20 ± 5 nm size. (c) A plot UV-visible spectrum of the used particles showing single symmetric absorption band with maximum peak of absorbance around ~400 nm which corresponds to the normal absorption spectrum of SNPs.
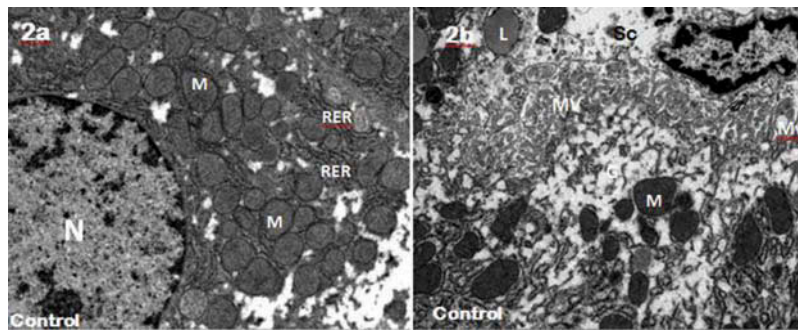
Figure 2. (a–b). Transmission electron micrographs of control rats demonstrating: (a) Control hepatocyte showing normal organelle ultrastructure with rounded nucleus (N), numerous of mitochondria (M), rough endoplasmic reticulum (RER), and bounded ribosomes. ×12,000. (b) Control heptocyte showing lipid droplets (L), glycogen particles (G), sinusoidal cell (Sc), and microvilli (Mv). ×15,000.
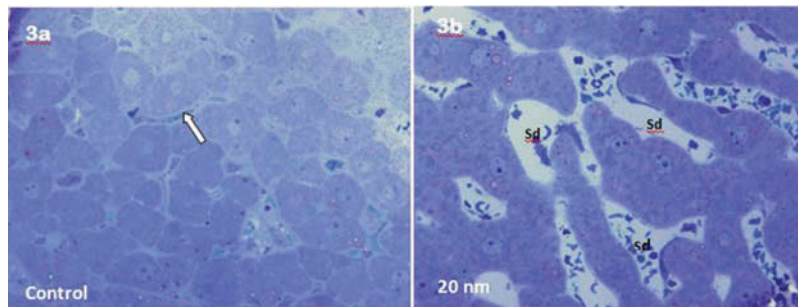

Figure 3. (a–b). Toluidine blue stained semithin sections of: (a) Control rat demonstrating normal sinusoids (arrow). ×1000. (b) SNP-treated rats demonstrating dilated sinusoids (Sd) with different architecture from that of the control rat indicating vascular lesion. ×1000.
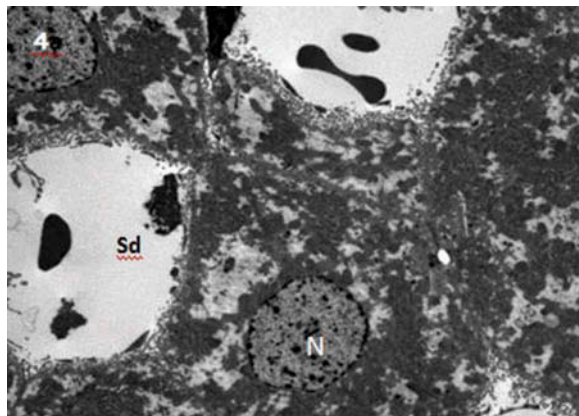

Figure 4. Transmission electron micrograph of SNP-treated rats demonstrating red blood cells and debris in the dilated sinusoids (Sd). ×4000.

angulations, and elongation along their longitudinal axis with occasional ruptured membranes (Figures 6a–c). Some swollen mitochondria were short and emarginated in comparison to well-preserved mitochondria in the control hepatocytes. In addition, some mitochondria demonstrate SNPs within their matrices.

- Cytoplasmic vacuolization: The cytoplasm of the affected hepatocytes appeared disorganized with variable sizes of cytoplasmic vacuoles (Figure 7).
- Lipid droplet accumulation: In comparison with the control hepatocytes, marked elevation number of variable sizes of lipid droplets was demonstrated in the cytoplasm of some affected hepatocytes (Figure 8).

- Glycogen depletion: In comparison with the control hepatocytes, evident glycogen depletion was clear in the hepatocytes of rat subjected to SNPs (Figure 9).
- Multilammellar body formation: Some affected cells demonstrated membranous phagolysosomes multi-layered myelin figures. Some of these bodies were embedded in cytoplasmic vacuoles (Figure 10).
- Nuclear alterations: Some hepatocytes of SNP-treated rats demonstrated heterochromatic micronuclei, karyopyknosis, nuclear membrane irregularity, and occasional apoptosis (Figures 11a–d).
- Multiple lysosomes: Hepatocytes of SNP-treated rats demonstrated multiple lysosomes some of which were membranous phagolysosomes (Figure 12).
- Kupffer cell alterations: Semithin and ultrathin sections of the hepatic tissue of SNP-treated rats demonstrated hypertrophoid Kupffer cells with irregular pyknotic nuclei (Figure 13). Some Kupffer cells showed vacuoles, multiple lysosomes, occasional phagocytic deposits, and minute electron-dense bodies.

Discussion

SNPs are important materials in industry and nanomedicine because of their unique biological and physiochemical characteristics. The results of the present work indicated that SNPs could induce variable ultrastructural alterations in most organelles of the hepatocytes. This finding is in consistence with some previous studies that indicated that the liver is a target organ for SNPs [28,29,31].
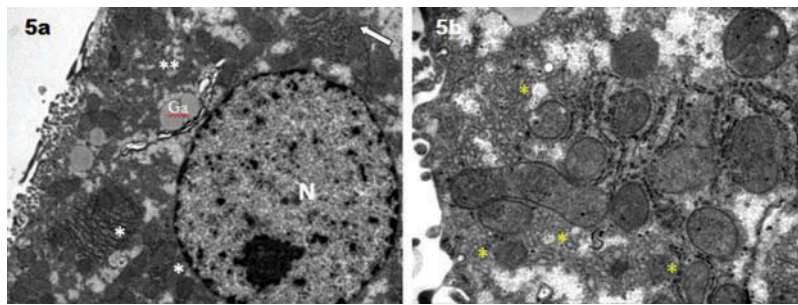
Figure 5. (a–b). Transmission electron micrographs of SNP-treated rats demonstrating: (a) Endoplasmic reticulum disruption (arrow), loss of array (*), ER reduction profile (**) and Golgi apparatus trans face (Ga). Note that the ER cisternae are broken up and fragmented. ×10,000. (b) Vesiculated endoplasmic reticulum (stars) that might indicate fluid ingress or storage products. ×30,000.
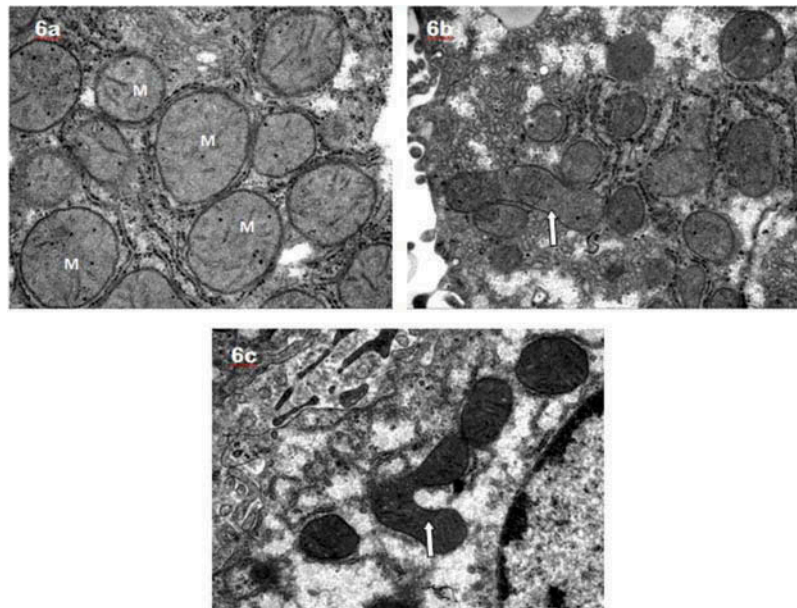

Figure 6. (a–c). Transmission electron micrographs of SNP-treated rats demonstrating: (a) Swollen mitochondria (M) with partial cristolysis. Note the lucent mitochondrial matrix and disarrangement of cristae. In addition, some mitochondria demonstrate SNPs (dark dots) within their matrices. ×40,000. (b) Elongated mitochondrium (arrow) along its longitudinal axis with other mitochondria exhibiting variable size and shape. ×30,000. (c) Angular mitochondrion (arrow). Note the rupture of the mitochondria cristae together with glycogen depletion in the cytoplasm of the demonstrated hepatocyte. ×30,000.
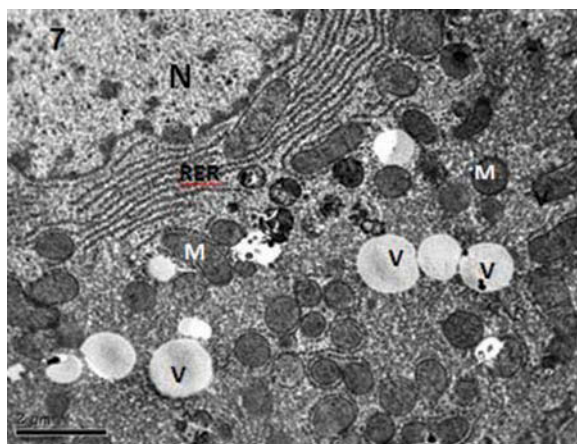

Figure 7. Transmission electron micrograph of SNP-treated rat demonstrating multiple cytoplasmic vacuoles (V) of different sizes. ×15,000.

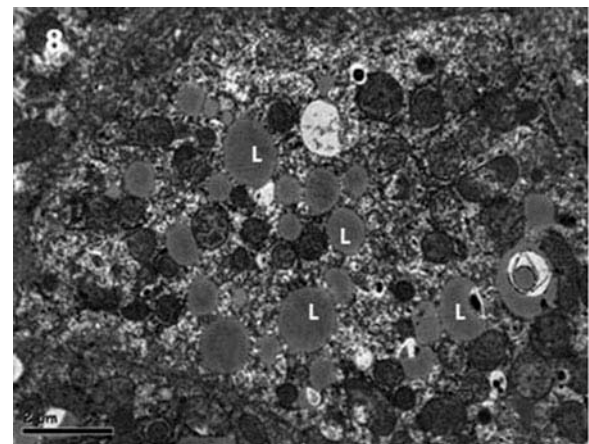**Figure 8.** Transmission electron micrographs of SNP-treated rat demonstrating numerous lipid droplets (L) occupying most of the cytoplasm. ×15,000.
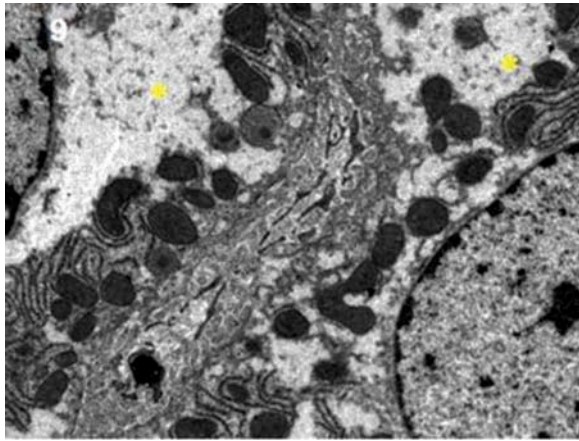
Figure 9. Transmission electron micrograph of SNP-treated rats demonstrating glycogen depletion (*). ×15,000.
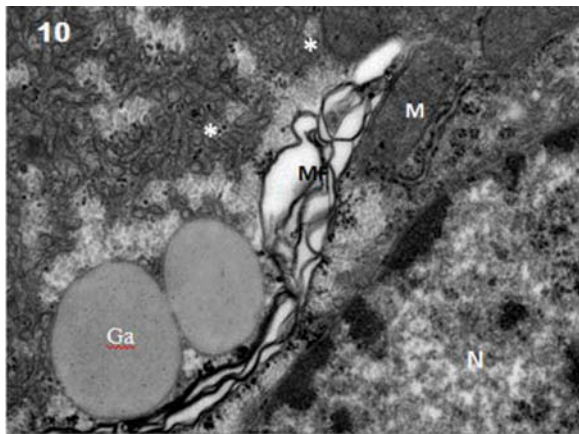

Figure 10. Transmission electron micrograph of SNP-treated rat demonstrating myelin figures (MF) in whorled arrays membranous structure. Note Golgi apparatus trans face (Ga) and dilated degranular rough ER (*) in the cytoplasm. ×40,000.

SNPs enter the cells by endocytosis targeting the organelles and deposited in the nucleus with probable consequence of oxidative damage to DNA. The results of the present study illustrated that the mitochondria were the most affected organelles by the toxicity of these particles. This is in agreement with other findings where Asharani et al. [25] reported that SNPs could penetrate into cellular organelles specially the mitochondria. The present study showed that mitochondrial damage was demonstrated in the form of swelling and crystolysis due to SNP exposure. These together might indicate alteration in the osmolarity of the hepatocyte causing salt influx to the mitochondrial matrix and affecting the integrity of the inner membrane. Mitochondrial cristae play an important role in the function of this organelle [46–48]. Crystolysis induced by SNPs might affect oxidative phosphorylation and ATP production due to the effect of these particles in the efficiency of the mitochondrial electron transport system [49–52]. The access of SNPs into the mitochondria may stimulate cytotoxicity by ROS generation. Several reports indicated that high level of ROS in the mitochondria could cause damage and depolarization in the mitochondrial membranes causing ATP synthesis interruption [53–54]. In addition, ROS generation by SNPs may affect the DNA repair, induce DNA damage, and activate the apoptotic gene P_{53}. Furthermore, some previous studies indicated that SNPs might induce metalothionin upregulation and heme oxygenase-1 gene upgrading as a defend mechanism of detoxification and protection from free radical stress induced by these particles [52–53]. Some investigators reported DNA damage in human mesenchymal stem cell after 1, 3, and 24 h exposure to SNPs at 0.1 μg/ml by both comet assay and aberration tests [49].

The results of the present work indicated that SNPs could affect hepatocyte rough ER in the form of destruction, loss of array, vesiculation, and stack shortening. This stress might be resulted due to hepatocyte redox disturbance in the ER
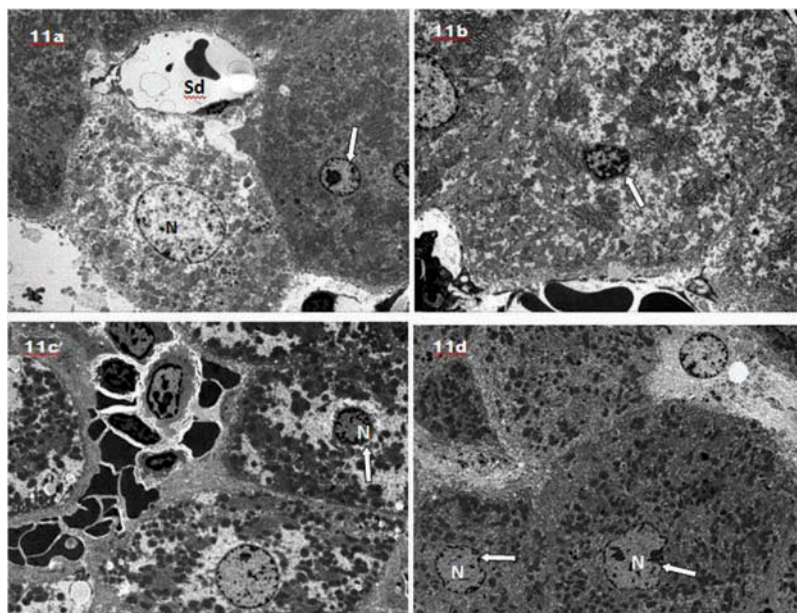

Figure 11. (a–d). Transmission electron micrographs of SNP-treated rats demonstrating hepatocytes with: (a) Micronucleus (arrow). Note the nucleus size ratio of the indicated hepatocyte with that of the hepatocyte on the left showing normal nucleus. ×3000. (b) Apoptotic hepatocyte (arrow). Note the formation of granular emarginated chromatin masses against the nuclear membrane. ×5000. (c) Karyopyknosis (arrow). Note chromatin condensation and nucleus shrinkage. ×3000. (d) Nuclear membrane irregularity (arrows). Note the difference from the smooth nuclear membrane of the control hepatocyte (Figure 2a). ×3000.
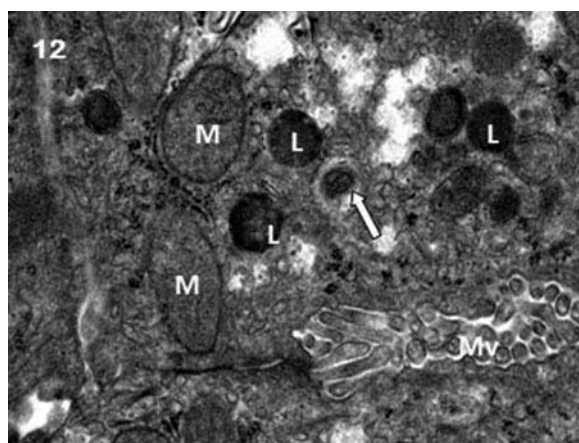
Figure 12. Transmission electron micrograph of SNP-treated rat demonstrating multiple lysosomes (L), phagolysosomes (arrow), mitochondrial crystolysis (M), and microvilli (Mv) in Disse's space. ×40,000.
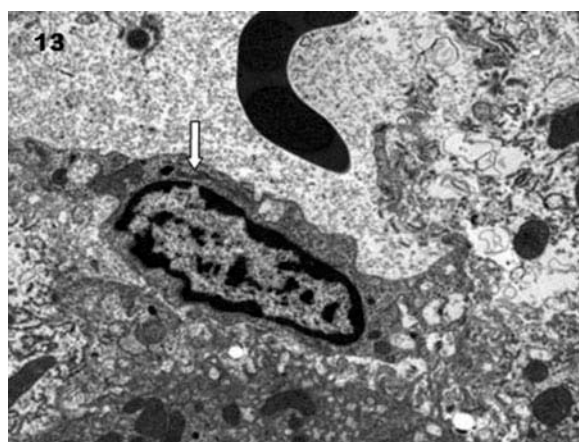

Figure 13. Transmission electron micrograph of SNP-treated rat demonstrating hypertrophoid Kupffer cell with irregular pyknotic nucleus (arrow). Note the phagocytized deposits in the cytoplasm. ×10,000.

membranes induced by SNPs. These together would indicate that SNPs would decrease the surface density of the endoplasmic reticulum that may negatively impact protein and lipid synthesis by the affected hepatocytes. Shannhan et al. [55] reported affinity of SNPs toward hydrophobic proteins for protein corona formation and electrostatic interaction. Recent studies indicated that SNPs always interact with cellular proteins forming corona prior to their biological action [24].

The hepatocytes of SNP-treated rats demonstrated partial glycogen depletion. This may indicate that the oxidative stress induced by SNPs may affect the activity of some enzymes necessary for glycogen synthesis. Moreover, lipid droplet accumulation in the cytoplasm of the affected hepatocytes might indicate impairment of fatty acid removal due to SNP toxicity or inability of the affected cells to catabolize fats. In addition, SNP exposure induced lysosomal autophagy which might indicate the need of the affected hepatocytes to degrade the foreign materials and damaged organelles. This finding is in consistence with some studies indicating lysosomal autophagy induced by nanotoxicity [56].

SNP exposure induced hepatocyte nuclear alterations including apoptosis. Some previous studies described apoptosis as major mechanism of cell death by oxidative stress of nanoparticles [20,57]. This programmed cell death might be resulted from the reduction of ATP production due to the mitochondrial damage induced by SNPs. One study showed that exposure of rats with single intraperitoneal dose of 2 mg/kg SNPs (100 nm diameter) induced apoptosis after 48 h of administration [58]. According to Kim et al. [59], SNPs could induce apoptosis by ROS generation via mitochondrial caspase-dependent pathways. Furthermore, some toxicological studies explained that SNP exposure could induce necrosis and gene alterations [60,61]. In addition, the findings of the current work showed that some hepatocytes of SNP-treated rats demonstrated micronuclei which is in consistence with the report of Song et al. [62]. Micronuclei formation is an indication of DNA damage, ultimately leading to cell death and usually seen in chemical induced genotoxicity.

The results of the present investigation revealed that SNPs could induce multilammellar body formation. Lamellar myelin figures were found to have lysosomal character consisting mainly of phospholipids, glucosylceramide, and lytic enzymes with autophagic activities. Formation of these figures might indicate pathologic hallmark of phospholipidosis and cytotoxicity associated with SNP exposure [63–65].

The present work demonstrated Kupffer cell hyperplasia due to SNP exposure. These cells are hepatic macrophages activated by subtoxic concentration of hepatotoxins and always demonstrated with liver injuries [66]. The activation and enlargement of these cells are always related with stress induced in the hepatic tissues by some drugs and environmental pollutants.

One would conclude from the results of the present study that exposure to SNPs would induce hepatocytes cytoplasmic and nuclear ultrastructural alterations might be associated to disturbance in the pro-oxidant/antioxidant of the hepatocytes system leading to cellular damage and affecting the function of the liver. In addition, the results of present work may raise the concerns about the potential risk on human health that might be related with numerous applications of SNPs. More work is needed to elucidate probable pathophysiological alterations and hepatotoxicity that might be resulted from SNP exposure.

Funding

References

1. Rai MK, Deshmukh SD, Ingle AP, et al. Silver nanoparticles: The powerful nanoweapon against multidrug resistant bacteria. *J Appl Microbiol* 2012;112:841–52.
2. Chou WL, Yu DG, Yang MC. The preparation and characterization of silver loading cellulose acetate hollow fiber membrane for water treatment. *Polym Adv Technol* 2005;16:600–7.
3. Kalantzi OI, Biskos G. Methods for assessing basic particle properties and cytotoxicity of engineered nanoparticles. *Toxics* 2014;2:79–91.

4. Qin Y. Silver-containing alginate fibers and dressing. *Int Wound J* 2005;2:172–6.

5. Jain J, Arora S, Rajwade J, et al. Silver nanoparticles in therapeutics: Development of an antimicrobial gel formulation for topical use. *Mol Pharm* 2009;6:1388–1401.

6. Vigneshwaran N, Kathe AA, Varada PV, et al. Functional finishing of cotton fabrics using silver nanoparticles. *J Nanosci Nanotechnol* 2007;7:1893–7.

7. Turtle GR. Size and Surface Area Dependent Toxicity of Silver Nanoparticles in Zebrafish Embryo (*Danio rerio*). Master Thesis in toxicology submitted to Oregon State University, USA, 2012.

8. Ahamed M, Alsalhi MS, Siddiqui MK. Silver nanoparticle applications and human health. *Clin Chem Acta* 2010;411:1841–8.

9. Faraj AH, Wipf P. Nanoparticles in cellular drug delivery. *Bioorg Med Chem* 2009;17:2950–2962.

10. Attia AA. Evaluation of the testicular alterations induced by silver nanoparticles in male mice: Biochemical, histological and ultrastructural studies. *RJPBSC* 2014;5(4): 1558–9.

11. Asharani PV, Hande MP, Valiyaveettil S. Anti-proliferative activity of silver nanoparticles. *BMC Cell Biol* 2009;10(65): 1–14.

12. Liu J, Hurt RH. Ion release kinetics and particle persistence in aqueous non-silver colloids. *Environ Sci Technol* 2010;44:2169–75.

13. Ahamed M, Posgai R, Gorey TJ, et al. Silver nanoparticles induced heat shock protein 70, oxidative stress and apoptosis in *Drosophila melanogaster*. *Toxicol Appl Pharmacol* 2010; 242: 263–9.

14. Lim D, Roh JY, Eom HJ, et al. Oxidative stress-related PMK- 1 P38 MAPK activation as a mechanism for toxicity of silver nanoparticles to reproduction in the nematode *Caenorhabditis elegans*. *Environ Toxicol Chem* 2012;31:585–92.

15. Park EJ, Bae E, Yi J, et al. Repeated-dose toxicity and inflammatory responses in mice by oral administration of silver nanoparticles. *Environ Toxicol Phar* 2010;30:162–8.

16. Park EJ, Yi J, Kim Y, et al. Silver nanoparticles induce cytotoxicity by a Trojan horse type mechanism. *Toxicol In Vitro* 2010;24:872–8.

17. Ma RC, Levard C, Marinakos SM, et al. Size-controlled dissolution of organic-coated silver nanoparticles. *Environ Sci Technol* 2012;46:752–759.

18. Schrand AM, Bradich-Stolle LK, Schlager JJ, et al. Can silver nanoparticles be useful as potential biological labels? *Nanotechnology* 2008;19:1–13.

19. Schrand AM, Rahman MF, Hussain SM, et al. Metal-based nanoparticles and their toxicity assessment. *WIREs Nanomed Nanobiotechnol* 2010;2:544–68.

20. Hsin YH, Chen CF, Huang S, et al. The apoptotic effect of nanosilver is mediated by a ROS- and JNK-dependent mechanism involving the mitochondrial pathway in NIH3T3 cells. *Toxicol Lett* 2008;179:130–9.

21. Carlson C, Hussian SM, Schrand AM, et al. Unique cellular interaction of silver nanoparticles: Size-dependent generation of reactive oxygen species. *J Phys Chem B* 2008;112:13608–19.

22. Kim TH, Kim M, Park HS, et al. Size-dependent cellular toxicity of silver nanoparticles. *J Biomed Mater Res* 2012;100:1033–43.

23. Cedervall T, Lynch I, Lindman S, et al. Understanding the nanoparticle-protein corona using methods to quantify exchange rates and affinities of proteins for nanoparticles. *Proc Natl Acad Sci USA* 2007;104:2050–5.

24. Duran N, Silveira CP, Marcela Duran M, et al. Silver nanoparticle protein corona and toxicity: A mini-review. *J Nanobiotechnol* 2015;13:55.

25. Asharani PV, Hande MP, Valiyaveettil S. Anti-proliferative activity of silver nanoparticles. *BMC Cell Biol* 2009;10: 65.

26. Dawson KA, Salvati A, Lynch I. Nanotoxicology: Nanoparticles reconstruct lipids. *Nat Nanotechnol* 2009;4:84–85.

27. Oberdörster G, Sharp Z, Atudorei V, et al. Translocation of inhaled ultrafine particles to the brain. *Inhal Toxicol.* 2004;16:437–45.

28. Jarrar Q. Silver Nanoparticles Toxicity: Size Effects. Thesis was submitted for Master Degree in Analytical Toxicology for the University of Jordan, 2013.

29. Sharma HS, Hussain S, Schlager J, et al. Influence of nanoparticles on blood–brain barrier permeability and brain edema formation in rats. *Acta Neurochir Suppl* 2010;106:359–364.

30. Dziendzikowska K, Gromadzka-Ostrowska J, Lankoff A, et al. Time-dependent biodistribution and excretion of silver nanoparticles in male Wistar rats. *J Appl Toxicol* 2012;32:920–8.

31. Jarrar Q, Battah A, Obeidat F et al. Biochemical changes induced by the toxicity of variable sizes of silver nanoparticles. *Brit J Pharmac Res* 2014;4(24): 2670–8.

32. Trop M, Novak M, Rodl S, et al. Silver-coated wound dressing acticoat caused raised liver enzymes argyria-like symptoms in burn patient. *J Trauma* 2006;60:648–52.

33. Almansour M, Jarrar Q, Battah A, et al. Histomorphometric alterations induced in the testicular tissues by variable sizes of silver nanoparticles. *J Rep Med* 2016; manuscript accepted for publication.

34. Seiffert J, Hussain F, Wiegman C, et al. Pulmonary toxicity of instilled silver nanoparticles: Influence of size, coating and rat strain. *Plos One.* 2015. doi:10.1371/journal.pone.0119726

35. Hussain SM, Hess KL, Gearhart JM, et al. In vitro toxicity of nanoparticles in BRl 3A rat liver cells. *Toxicol In Vitro* 2005;19:975–83.

36. Oberdörster G, Stone V, Donaldson K. Toxicology of nanoparticles: A historical perspective. *Nanotoxicology* 2007;1:2–25.

37. Kim YS, Song MY, Park JD, et al. Subchronic oral toxicity of silver nanoparticles. *Part Fibre Toxicol.* 2010;7: 20.

38. Johnston HJ, Hutchison G, Christensen FM, et al. A review of the in vivo and in vitro toxicity of silver and gold particulates: Particle attributes and biological mechanisms responsible for the for the observed toxicity. *Crit Rev Toxicol.* 2010;40:328–46.

39. Xue Y, Zhang S, Huang Y, et al. Acute toxic effects and gender-related biokinetics of silver nanoparticles following an intravenous injection in mice. *J Appl Toxicol* 2012;32:890–9.

40. Austin CA, Umbreit TH, Brown KM, et al. Distribution of silver nanoparticles in pregnant mice and developing embryos. *Nanotoxicology* 2011;6:912–922.

41. Farkas B, Geretovszky ZS. On determining the spot size for laser flounce measurements. *Appl Surf Sci* 2006;252:4728–32.

42. Bozzola, JJ, Russell LD. *Electron Microscopy: Principles and Techniques for Biologists*. 2nd ed. Boston: Jones and Bartlett, 1999.

43. Mascorro JA, Bozzola JJ. Processing biological tissues for ultra-structural study. In: *Electron microscopy, methods and protocols. Methods in molecular biology*. Ed. John Kuo. Human Press, 2007, pp. 19–34.

44. Ayache J, Beaunier L, Boumendil J, et al. Sample *preparation handbook for transmission electron microscopy, methodology*. London: Springer Press, 2010.

45. Hayat MA. *Principles and techniques of electron microscopy, biological applications*. 4th ed. Cambridge: Cambridge University Press, 2000.

46. El-Shenawy NS. Oxidative stress responses of rats exposed to roundup and its active ingredient glyphosate. *Environ Toxicol Pharmacol* 2009;28:379–85.

47. Braydich-Stolle L, Hussain S, Schlager JJ, et al. In vitro cytotoxicity of nanoparticles in mammalian germline stem cells. *Toxicol Sci* 2005;88:412–9.

48. Singh A, Bhat T, Sharma OP. Clinical biochemistry and hepato-toxicity. *J Clin Toxicol* 2011;4:11–8.

49. Gurabi M, Ali D, Alkahtani S, et al. In vivo DNA and apoptotic potential of silver nanoparticles in Swiss albino mice. *Onco Targets Ther* 2015;8:295–302.

50. Shlan MG, Mostafa MS, Hassouna MM, et al. Elrafaie. Amelioration of lead toxicity on rat liver with vitamin C and silymarin supplements. *Toxicology* 2005;206(1): 1–15.

51. Sioutas C, Delfino RJ, Singh M. Exposure assessment for atmospheric ultrafine particles (UFPs) and implications in epidemiologic research. *Environ Health Perspec* 2005;113(8): 947–55.

52. Xia T, Kovochich M, J. Brant, et al. Comparison of the abilities of ambient and manufactured nanoparticles to induce cellular toxicity according to an oxidative stress paradigm. *Nano Lett* 2006;6(8): 1794–807.

53. Lenaz G. The mitochondrial production of reactive oxygen species: Mechanisms and implications in human pathology. *IUBMB Life* 2001;52(3–5): 159–64.

54. Buko V, Ergov A, Karput S, et al. Mitochondrial respiration and oxidative phosphorylation in thioacetamide-induced liver necrosis. *Toxicol Lett* 1998;95:162–162.

55. Shannahan JH, Lai X, Ke PC, et al. Silver nanoparticle protein corona composition in cell culture media. *Plos One* 2013;8: e74001

56. Stern ST, Adiseshaiah PP, Crist RM. Autophagy and lysosomal dysfunction as emerging mechanisms of nanomaterial toxicity. *Part Fibre Toxicol* 2012;9: 20

57. Eom E, J. Choi J. p38 MAPK activation, DNA damage, cell cycle arrest and apoptosis as mechanisms of toxicity of silver nanoparticles in Jurkat T cells. *Environ Sci Technol* 2010;44(21): 8337–42.

58. Serhan OM, Hussein RM. Effects of intraperitoneally injected silver nanoparticles on histological structures and blood parameters in the albino rat. *Int J Nanomed* 2014;9:1505–16.

59. Kim S, Kim S, Lee S, et al. Characterization of the effects of silver nanoparticles on liver cell using HR-MAS NMR spectroscopy. *Bull Korean Chem Soc* 2011;32(6): 2021–6.

60. Asharani, PV, Wu YL, Gong Z, et al. Toxicity of silver nanoparticles in zebra fish models. *Nanotechnology* 2008;19(25): 255102.

61. Bouwmeester H, Poortman J, Peters RJ et al. Characterization of translocation of silver nanoparticles and effects on whole-genome gene expression using an in vitro intestinal epithelium coculture model. *ACS Nano* 2011;5:4091–103.

62. Song MF, Li YS, Kasai H, et al. Metal nanoparticle-induced micronuclei and oxidative DNA damage in mice. *J Clin Biochem Nutr* 2012;50(3): 211–6.

63. Urich RG, Cramer CT. Potential to induce lamellar bodies and acute cytotoxicity of 6'-alkyl analogues of spectinomycin in primary cultures of rat hepatocytes. *Toxicol In Vitro* 1991;5(3): 239–245.

64. Schmitz G, Muller G. Structure and function of lamellar bodies, lipid-protein complexes involved in storage and secretion of cellular lipids. *J Lipid Res* 1991;32:1539–70.

65. Anderson N, Borlak J. Drug-induced phospholipidosis. *FEBS Lett* 2006;580(23): 5533–40.

66. Kegel V, Pfeiffer E, Burkhardt B, et al. Subtoxic concentrations of hepatotoxic drugs lead to Kupffer cell activation in a human in vitro liver model: An approach to study DILI. *Mediat Inflamm* 2015; Article ID 640631.